Macromolecular Research Article

DOI 10.1007/s13233-018-6112-2 www.springer.com/13233 pISSN 1598-5032 eISSN 2092-7673

BSA/Chitosan Polyelectrolyte Complex: A Platform for Enhancing the Loading and Cancer Cell-Uptake of Resveratrol

Marjan Ghorbani[1]
Hamed Hamishehkar*[,2]
Mahnaz Tabibiazar*[,3]

[1] Stem Cell Research Center, Tabriz University of Medical Sciences, Tabriz, Iran
[2] Drug Applied Research Center, Tabriz University of Medical Sciences, Tabriz, Iran
[3] Nutrition Research Center, and Department of Food Science and Technology, Faculty of Nutrition, Tabriz University of Medical Sciences, Tabriz, Iran

Received December 22, 2017 / Revised March 10, 2018 / Accepted March 17, 2018

Abstract: The ultimate goal of cancer therapy is to kill as many cancerous cells while minimizing damage to the normal cells nearby. However, conventional chemotherapy suffers from drug resistance and lack of selectivity and consequently increased side effects which all can be overcome by application of nanocarriers. Resveratrol (Res) is supposed to act as a chemo-preventive agent by various mechanisms but its low chemical stability and restricted bioavailability limit its therapeutic application. To afford of these limitations, Res-loaded bovine serum albumin (Res-BSA) nanocarrier was developed. Then, to elevate the cytotoxic performance of Res-BSA, chitosan (CS) was used to provide adequate positive charge on the surface of nanoparticles and consequently cause enhanced cell-uptake. The particle size of Res-BSA/CS (235 ±11 nm) showed narrow distributed nano-ranged size (PdI: 0.095) and the amount of complexed Res with NPs was found to be approximately 65% in BSA/CS complex. The successful cell uptake of Res-BSA/CS was investigated *via* fluorescence microscopy and flow cytometry and the results showed that Res-BSA/CS induced 1.5 times more cell internalization than Res-BSA. Consequently, cell cytotoxicity studies pointed out ~1.5 and 3 times higher cell cytotoxicity after 24 h and 48 h for Res-BSA/CS than Res in MTT assay. Thus, it can be concluded that the developed Res-loaded BSA/CS nanocarrier paves a way for efficient cancer therapy and may be considered as an attractive and promising approach to enhance the therapeutic performance of Res against cancer.

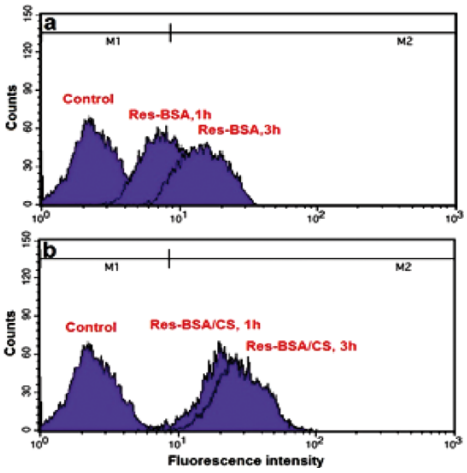

Keywords: bovine serum albumin, chitosan, drug delivery, nanoparticle, resveratrol.

1. Introduction

Trans-Resveratrol (Trans-Res) (3,5,4′-trihydroxystillbene) is a non-flavonoid polyphenolic compound found naturally in at least 72 plant species, such as grapes, peanuts, berries, and cacao.[1] The Res healthy effects such as cardio-protective,[2] antioxidant,[3] anti-inflammatory,[4] anti-allergenic,[5] neuro-protective[4] and anti-aging[6] properties were reported in many studies. Recently, Res has been revealed to have a potent chemo-preventive effect in multiple carcinogenesis models to inhibit the growth of several types of cancers. Thereafter, many studies have exposed anti-cancer properties of Res in various human cancers including stomach,[7] skin,[8] breast,[9] lung,[10] prostate,[11] liver,[12] and colon.[13] However, Res has limited solubility in water and extreme photosensitivity which restrict its beneficial effect.[14] For this purpose, nanotechnology provides a plausible pharmaceutical basis for enhancing oral bioavailability and therapeutic effectiveness of these compounds by creating stable colloids to protect them from photon and target it to the cancerous tissue by intravascular administration by means of enhanced permeability and retention (EPR) effect.[15-18] Thus, with complexation between Resveratrol (RES) and bovine serum albumin (BSA), BSA can act as a nanocarrier for RES because of its availability, high purity, low cost, high aqueous solubility.[19,20] Additionally, to increase the intracellular delivery of the nanocarriers, it is valuable to develop strategies that can internalize nanoparticles (NPs) better through endocytosis process.[21,22] Endocytosis is a distinct process to take up macromolecules and NPs from the surrounding medium into the cells which has been accelerated by positive charge macromolecules and NPs. Among the cationic polymers, chitosan (CS) has attracted interest as a biocompatible, biodegradable, mucoadhesive, and nontoxic material for use in food and drug industries.[23,24] Colloidal polyelectrolyte complexes are macromolecules with ionizable or ionic groups that mostly water-soluble and exhibit unique properties mainly attributed to their electrostatic interactions and flexibility. Therefore, in this work, BSA, an endogenic protein was used for complexation with Res, and CS used for polyelectrolyte complexation with this nanocarrier to provide enough external cationic charge for proper cell internalization of nanocarrier and anti-cancer

Acknowledgments: The support of Drug Applied Research Center, Tabriz University of Medical Sciences were gratefully acknowledged.

***Corresponding Authors:** Hamed Hamishehkar (hamishehkarh@tbzmed.ac.ir or hamishehkar.hamed@gmail.com),
Mahnaz Tabibiazar (mahnaz_tabibiazar@yahoo.com)

performance of Res. The developed nanoelectrolyte carrier can offer a novel platform for passive targeting of various hydrophobic anti-cancer agents.

2. Experimental

2.1. Materials

Low molecular-weight chitosan (poly D-glucosamine) with a high degree of deacetylation>75%, lyophilized BSA, trans-Res (3, 4′, 5-trihydroxystillbene, >99% pure), 3-(4,5-dimethyl-2-thiazolyl)-2,5-Diphenyltetrazolium bromide (MTT), fluorescein dye and polyethylene glycol (PEG, average molecular weights of 400 Da) were purchased from Sigma Aldrich (USA).

2.2. Preparation of NPs

BSA and CS solutions were prepared both in the concentration of 5 mg/mL in distilled water and acetic acid 3% w/w, respectively. The low concentration of biopolymer was critical factor in formation of NPs. Different concentration of CS was added to BSA and the pH of mixed solution was adjusted in 5.4. BSA/CS solution was stirred in 500 rpm at 40 °C for 120 min to complete interaction. Based on colloidal stability appearance and particle size results, the most stable formulation was selected for loading of Res. Res was solubilized in PEG and was added to BSA solution and BSA/CS solution incubated overnight. The final concentration of Res was kept constant in all formulation (730 mM). All vials were covered with aluminums foil to protect against the photochemical degradation of Res and stored in refrigerate.

2.3. Complexation efficiency

Complexation efficiency (CE) of Res in NPs was assessed using Amicon® centrifugal filter (Millipore, MW cut off 100 kDa).[25] A volume of 1 mL of the Res-BSA solution was mixed with 1 mL of ethanol to solubilize unloaded Res. Then this dispersion of Res-loaded NPs was placed on the upper compartment of Amicon® tubes and centrifuged at 4000 rpm for 30 min to separate free Res from the lower compartment of Amicon®. After proper dilution of filtrate sample with mobile phase, 50 µL of this mixture was injected into high-performance liquid chromatography-ultraviolet (HPLC-UV) to determine Res concentration. HPLC-UV analysis was carried out on a Knauer (Germany) system equipped with a UV–visible detector (K-2600, Knauer, Germany), a pump (K-1001, Knauer, Germany), and a Knauer injector consisting of a 20 µL loop. The separation was performed on an analytical C_{18}-column (5 µm particle diameter, 4.6 mm i.d ×25 cm) (Knauer, Germany) at room temperature. The mobile phase of the methanol/phosphate buffer solution (10 mM) at a ratio of 63/37 (V/V) and the final pH adjustment of 6.8 were utilized in the isocratic mode at a flow rate of 1 mL/min. The peak for t-Res was detected at 306 nm by UV detector, and the calibration curve was provided with Res solution (1-75 µM in ethanol 50%v/v). The CE was calculated, using the following formula:

$$CE\ (\%) = \frac{\text{Total resveratrol - Free resveratrol}}{\text{Total resveratrol}} \times 100$$

2.4. Fourier transform infrared spectrometry (FTIR) analysis

FTIR spectra of BSA and CS powder and freeze-dried samples in KBr pellets were recorded (Tensor27, Bruker, Germany). Interferograms were accumulated over the spectral range of 500-4000 cm^{-1} with nominal resolution of 2 cm^{-1} and 100 scans. The freeze-drying process was performed at the temperature of -30 °C and the pressure of 0.07-0.1 mbar for 48 h in a (FD-10, Pishtaz Engineering, iran) freeze drier.

2.5. Scanning electron microscopy

The morphology and structure of NPs were visualized using scanning electron microscope (SEM). To perform scanning electron microscopy, freeze-dried samples were mounted on aluminum stubs. Subsequently, they were gold coated in vacuum by a sputter (SC7620-CF, Quorum Technologies, UK). The samples were observed by (KYKY-EM3200, Bio-equip, China) microscope at excitation voltage of 26 KV.

2.6. Particle size and zeta potential measurement

The particle size, poly-dispersity index (PDI) and zeta potential of samples were conducted using a Zetasizer (Nano ZS, Malvern Instruments, UK). Particle size measurements were done based on dynamic light scattering. This instrument determines the particle size distribution by measuring the intensity fluctuations over time of a laser beam (633 nm) scattered by the sample at an angle of 173°. Zeta potential measurements were executed based on laser Doppler anemometry, using the same machine. The samples were loaded into pre-rinsed folded capillary cells and a minimum of three measurements were made per sample for zeta potential measurements.

2.7. Cell biocompatibility and cytotoxicity studies

To assess the therapeutic ability of the NPs, the cytotoxicity of the Res-BSA and Res-BSA/CS NPs and the biocompatibility of the developed BSA/CS NPs were considered by MTT assay test against human breast adenocarcinoma (MCF-7) and healthy normal human umbilical vein endothelial (HUVEC) cell lines purchased from NCBI (National Cell Bank of Iran, Pasteur Institute). The cells were maintained in RPMI1640 with 10% fetal bovine serum at 37 °C in 5% CO_2. After incubation (VO400, Memmert, Germany) for 24 h, the culture medium was removed, and 200 µL growth mediums containing various concentrations of free Res, Res-BSA and Res-BSA/CS NPs were added to each well and incubated for 24 h and 48 h. Then, the medium containing NPs was exchanged with a 150 µL of fresh medium and 50 µL aliquots of MTT solution (5 mg/mL) for further 4 h incubation. The optical density (OD) values were measured at 570 nm with a background correction at 630 nm using a micro-plate reader (Elx808, Biotek, USA), and the results were compared with respect to control cells.

2.8. Cellular uptake study

To investigate the cellular uptake of NPs, fluorescein-labelled

NPs were prepared.[26] Fluorescein (5 mg) was dissolved in 1 mL of DMSO and 0.2 mL of the solution was added to 1 mL of 10 mg/mL of NPs. Then, 1 mL of 1 M sodium carbonate/sodium bicarbonate (Na_2CO_3/$NaHCO_3$) buffer was added to the suspension and stirred for 12 h. The excess fluorescein was separated by the Amicon® filter (molecular weight cutoff 100 kDa, Millipore, UK) followed by washing with double distilled water several times. Then, the cells (5×10^4 cells/mL) were seeded in each well and were incubated for 24 h in six-well plates. When the cells reached 90% confluence, the medium was removed and the cells were treated with fluorescein-labelled NPs (BSA and BSA/CS) for 4 h incubation. Then, the medium was removed and the cells were washed twice with 2 mL of PBS. Fluorescein uptake was measured using a FACS calibur flow cytometer (Becton Dickinson Immunocytometry Systems, San Jose, CA)

2.9. Cellular internalization study

The internalization of NPs in the cells was assessed using fluorescence microscopy imaging (Bh2-RFCA, Olympus, Japan). MCF-7 cells were seeded onto glass coverslips placed in six-well plates at 5×10^5 cells/well and then treated with fluorescein-labelled NPs for 1 h and 3 h. The coverslips were fixed onto the glass microscope slides and the cell penetration of NPs were observed using an inverted fluorescence microscopy.

2.10. Statistical analysis

All the experiments were performed three times independently with triplicates, and the results were expressed as mean ± standard deviation. The statistical analysis was carried out, using Graph Pad Prism software to find the statistical significance of these values. A probability of $p<0.05$ was considered statistically significant.

3. Results and discussion

3.1. Characterization of NPs

Res has low solubility in water, therefore a good solvent is required for achieving the desired homogeneity and consequently acceptable loaded of Res in NPs. PEG acts as a co-solvent and leads to an apparent decrease of polarity and dielectric constant of aqueous solutions.[27] The decrease in dielectric constant of solvent affects the interactions between oppositely charged polyelectrolyte.[28,29] To improve the cancer cell-uptake of Res-BSA NPs, the low molecular weight of CS was used. The mechanism of formation BSA/CS complex involves electrostatic attractive force between negatively charged BSA and positively charged CS.[30] Regarding to pKa value of CS (pK_a=6.5), amino groups of CS is protonated under lower pH conditions (pH<6.7). BSA as an anionic polymer has a negative charge above the isoelectric point (PI=4.7). Therefore, in the range of pH 4.7 and 6.5, existence of strong electrostatic attractive force between BSA and CS was caused to the formation of polyelectrolyte complexes. Moreover, for achieving a colloidal stable complex, we need to achieve optimum mole ratio of BSA to CS. In preliminary experiment in the points of size, zeta and colloidal stability, the most suitable ratio of BSA:CS was found to be 3:1 (pH=5.4). This is in line with previous study.[30] The visible opalescence was formed during the addition of high concentration of CS to the BSA solution. This observation was important because the colloidal stability is the main criterion in NPs preparation. A main factor for *in vivo* performance is the size of the NPs that is well within the favorite range of NPs (10-300 nm) for effective drug delivery *via* passive targeting.[31] The NPs are in suitable size range for passive targeted drug delivery to infiltrate into leaky cancerous tissues. As shown in Figure 1(a) and 1(b), the particle size of Res-BSA, and Res-BSA/CS were 21±8, and 235±11 nm, respectively. As shown in Figure 1(c), and 1(d), SEM images exhibited the large popu-

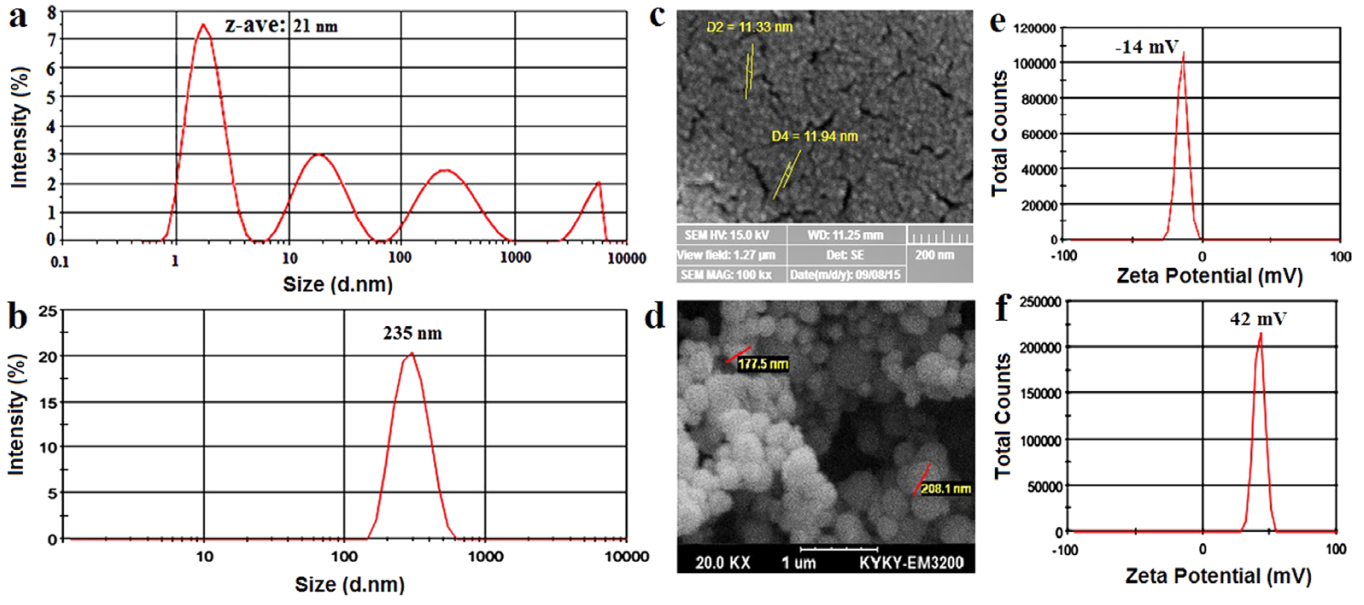

Figure 1. Size profiles of Res-BSA nanoparticles (NPs) (a) and Res-BSA/CS NPs (b), scanning electron-microscopy (SEM) images of Res-BSA NPs (c) and Res-BSA/CS NPs (d) and Zeta potentials of Res-BSA NPs (e) and Res-BSA/CS NPs (f).

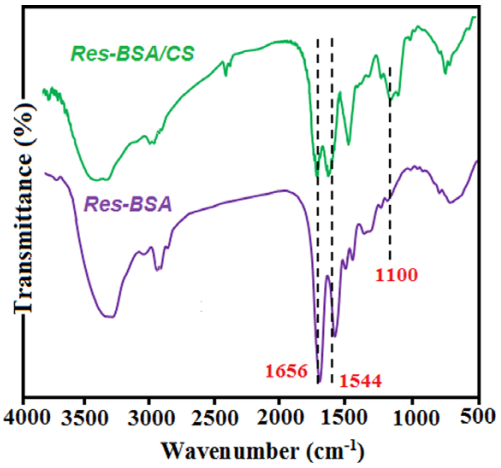

Figure 2. Fourier transform infrared spectroscopy (FT-IR) spectra of Res-BSA and Res-BSA/CS.

lation of particles in the field which confirmed the interpretation of PCS pattern. Additionally, it was reported that the zeta potential value of ±30 mV improved the long-term stability of dispersed nanoparticles.[32] The zeta potentials values for Res-BSA, and Res-BSA/CS complex were -14, and +42.1 mV in PBS (pH 7.4, 10 mM) *i.e.* physiological pH, respectively (Figure 1(e) and 1(f)).

The accuracy of chemical structure of NPs was confirmed by using the FTIR spectra (Figure 2). As shown in the FTIR spectrum of Res-BSA NPs, the absorbance at 1656 cm^{-1}, and 1544 cm^{-1} are assigned to the stretching vibration of C=O (amide band I) and bending vibration of N-H (amide band II), respectively, which belong to the characteristic peaks of BSA molecules.[33] Furthermore, the stretching vibration of the C-N groups appeared at 1280 cm^{-1} and the absorption peaks of C-O in CS appeared at about 1100 cm^{-1}. The amount of complexed Res with NPs was calculated to be approximately 65% in BSA/CS complex.

3.2. *In vitro* cell biocompatibility and cytotoxicity

An MTT assay was used to estimate the cell viability of MCF-7 and HUVEC cells to assess the therapeutic effect of the developed NPs. As shown in Figure 3(a) and 3(b), the cell viability of BSA and BSA/CS NPs showed no significant toxicity on viability of MCF-7 (as cancer cell line) and HUVEC (as normal cell line) cells after 24 h and 48 h, confirming that the NPs exhibited a good biocompatibility. In comparing the cytotoxicity profiles of the free Res with Res-BSA and Res-BSA/CS, Res-loaded NPs showed higher cell cytotoxicity than free form of drug after 24 h and 48 h against MCF-7 cell lines which would be valuable in lowering the administration dose of anticancer drugs (Figure 4). These results showed that the BSA and BSA/CS have many favorable potentials as drug carriers and offer an efficient anticancer delivery system. Furthermore, as reported in the literatures, the uptake of NPs with positive surface charge into cancer cells was greater than that of the NPs with no neutral and negative surface charge. Therefore, the ability of the Res-BSA/CS NPs in destroying the MCF-7 cells in more degrees than Res-BSA NPs was due to the better cellular uptake of BSA/CS NPs for the existence of positive surface charge of NPs.

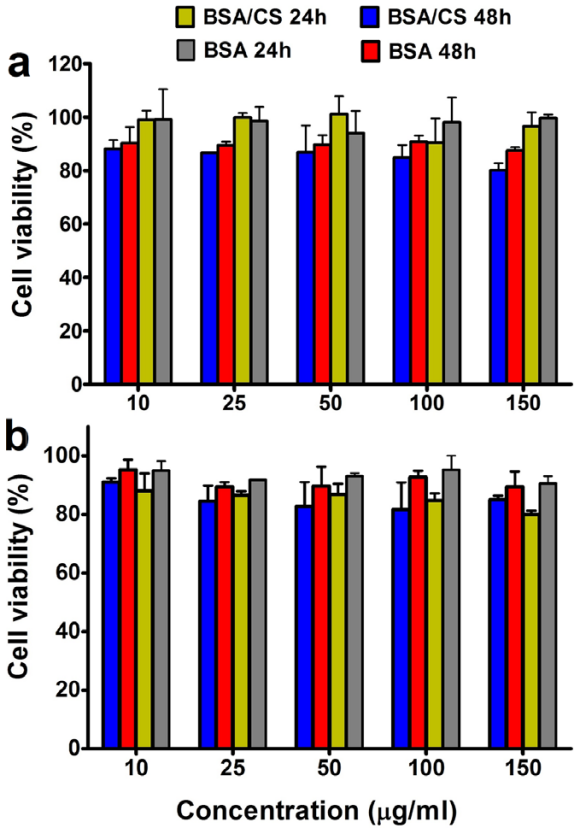

Figure 3. Biocompatibility of BSA and BSA/CS nanoparticles against human breast epithelial adenocarcinoma (MCF-7) (a) and healthy normal human umbilical vein endothelial (HUVEC) (b) cell lines for 24 h and 48 h.

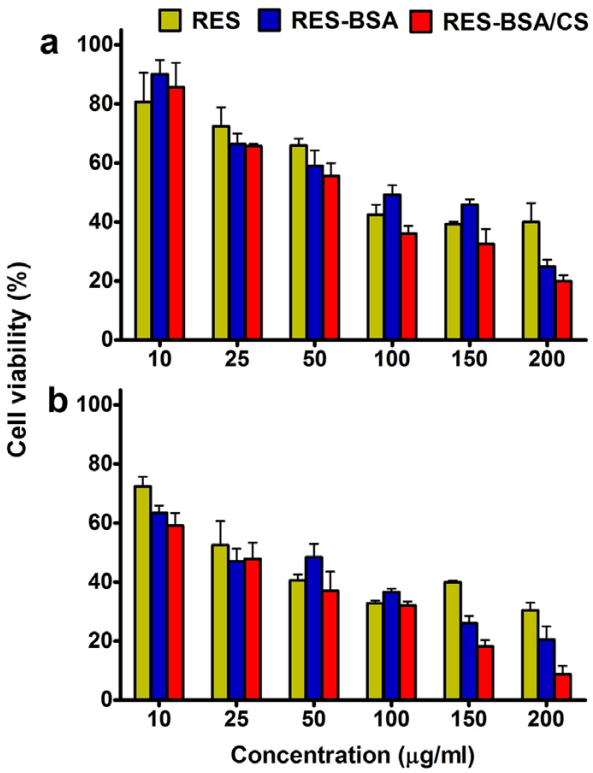

Figure 4. Cell viability study of Res, Res-BSA and Res-BSA/CS against human breast epithelial adenocarcinoma (MCF-7) after incubation for 24 h (a) and 48 h (b).

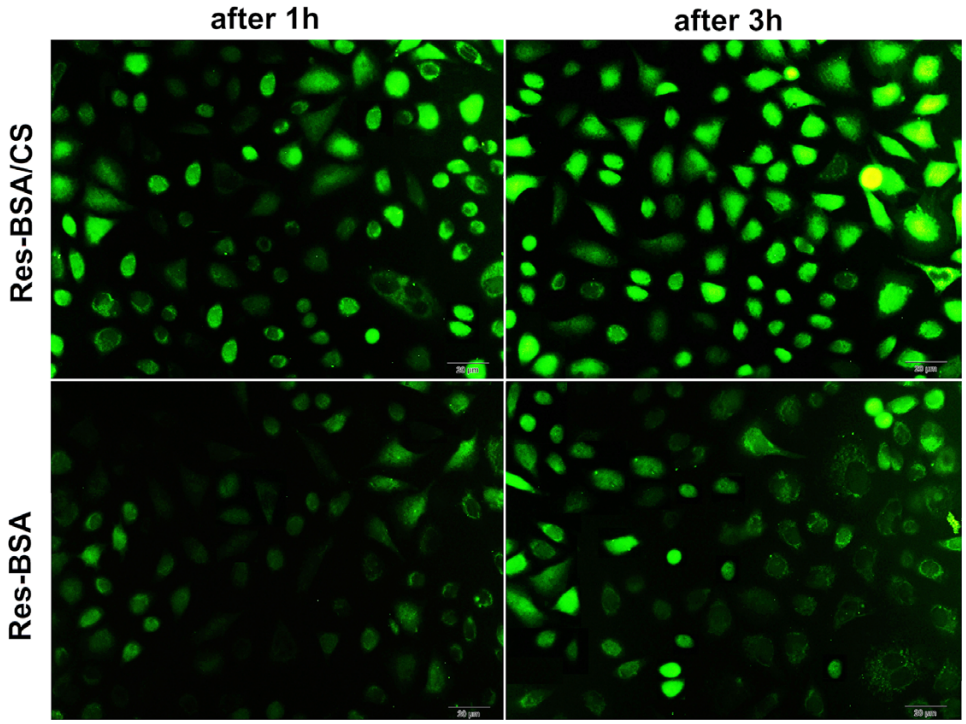

Figure 5. Fluorescence microscopy images of treated human breast epithelial adenocarcinoma (MCF-7) cells with Res-BSA and Res-BSA/CS after 1 h and 3 h.

3.3. Cell internalization assessment

3.3.1. Fluorescence microscopy

To interpret the MTT assay results, the cellular internalization of these NPs was visually considered and compared by a fluorescence microscopic (Figure 5). Physicochemical properties such as particle size and surface charge would influence NPs cell uptake. As shown in Figure 5, the cellular uptake extent of Res-BSA/CS NPs was considerably higher than those of Res-BSA NPs in MCF-7 cells which characterized by higher fluorescent intensity of Res-BSA/CS NPs than Res-BSA NPs after 1 h and 3h, indicating the effective performance of CS (as cationic polymer) in directing the NPs into the cells. Furthermore, enhanced fluorescence intensity was observed for both of NPs which proposed that NPs were competently transported into tumor cells during 3 h.

3.3.2. Flow cytometry

The *in vitro* cellular internalization of NPs was studied by flow cytometry to quantify the cell uptake ability of Res-loaded NPs. As shown in Figure 6, fluorescein labelled NPs (BSA and BSA/CS NPs) displayed a high fluorescence intensity, verifying that both of NPs were capable to efficiently internalize in MCF-7 cells after 1 h and 3 h. The higher cellular uptake into MCF-7 cells was observed for fluorescein labelled-BSA/CS NPs than fluorescein labelled-BSA NPs which is correspondence to the difference in surface charge. It is known that the cellular penetration rate of the nanocarriers depending on the interaction of the NPs and the surface charge of cell membrane, so the positively-charged NPs could be easily interacted with the negative cell surface, then the adsorbed BSA/CS NPs were internalized higher than that of BSA NPs which have negative surface charge.

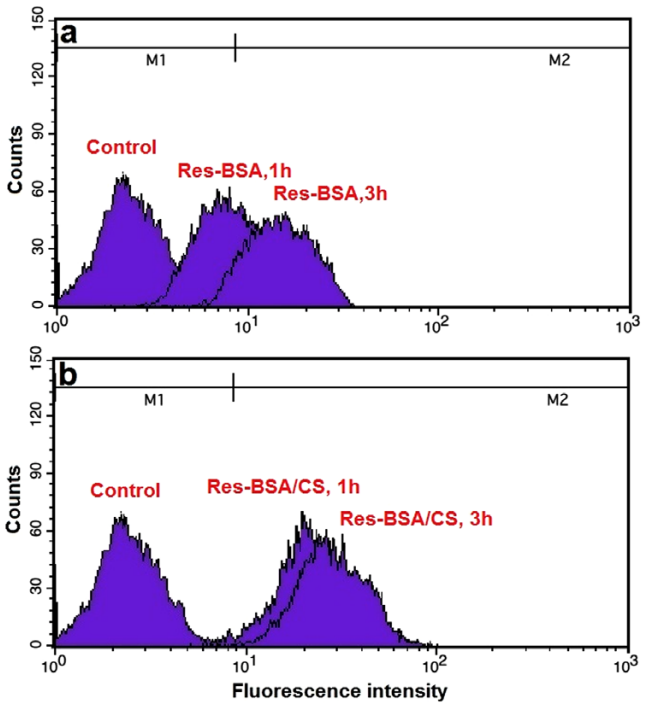

Figure 6. Cell uptake study of Res-BSA (a) and Res-BSA/CS nanoparticles (b) after incubation with human breast epithelial adenocarcinoma (MCF-7) cell line for 1 h and 3 h.

4. Conclusions

This study was assumed to assess the potential of complex formation between Res-BSA as a primary step for designing delivery system in cancer therapy. We have revealed Res solubility increased as function of BSA concentration up to 2.3:1 molar

ratio. Colloidal nanodispersion of Res-BSA complex (z-average =20 nm) was stable for more than 30 days. MTT experiment showed enhanced cytotoxic effect of Res-BSA complex compared to Res against cancer cell line. To improve the cell penetration of Res-BSA, CS (a positively charged polymer) was applied to coat the Res-BSA and the amount of encapsulated Res in BSA/CS complex was calculated to be 65%. The results of MTT assay specified that BSA/CS complex overcome negligible toxicity while the cytotoxicity of BSA/CS loaded Res was higher than Res alone after 24 and 48 h. Moreover, the conjugation of CS could improve the cell cytotoxicity and cellular uptake of developed NPs and these successful results of our approach was detected by flow-cytometry and cell imaging techniques. It was concluded that our newly developed Res-BSA-CS NPs may offer a new horizon in targeting drug delivery and pave a way for efficient cancer therapy.

References

(1) V. Katalinić, S. S. Možina, D. Skroza, I. Generalić, H. Abramovič, M. Miloš, I. Ljubenkov, S. Piskernik, I. Pezo, P. Terpinc, and M. Boban, *Food Chem.*, **119**, 715 (2010).

(2) L. M. Hung, J. K. Chen, S. S. Huang, R. S. Lee, and M. J. Su, *Cardiovasc. Res.*, **47**, 549 (2000).

(3) C. K. Singh, I. A. Siddiqui, S. El-Abd, H. Mukhtar, and N. Ahmad, *Mol. Nutr. Food Res.*, **60**, 1406 (2016).

(4) N. Steiner, R. Balez, N. Karunaweera, J. M. Lind, G. Munch and L. Ooi, *Neurochem. Int.*, **95**, 46 (2016).

(5) V. Trotta, W. H. Lee, C. Y. Loo, P. M. Young, D. Traini, and S. Scalia, *Eur. J. Pharm. Sci.*, **86**, 20 (2016).

(6) N. Calabriso, E. Scoditti, M. Massaro, M. Pellegrino, C. Storelli, I. Ingrosso, G. Giovinazzo, and M. A. Carluccio, *Eur. J. Nutr.*, **55**, 477 (2016).

(7) Z. Wang, W. Li, X. Meng, and B. Jia, *Clin. Exp. Pharmacol. Physiol.*, **39**, 227 (2012).

(8) K.-A. Lee, Y.-J. Lee, J. O. Ban, Y.-J. Lee, S.-H. Lee, M.-K. Cho, H.-S. Nam, J. T. Hong, and J.-H. Shim, *Int. J. Mol. Med.*, **30**, 21(2012).

(9) C. M. Deus, T. L. Serafim, S. Magalhães-Novais, A. Vilaça, A. C. Moreira, V. A. Sardão, S. M. Cardoso, and P. J. Oliveira, *Arch. Toxicol.*, **1** (2016).

(10) C.-L. Chen, Y. Chen, M.-C. Tai, C.-M. Liang, D.-W. Lu, and J.-T. Chen, *Drug Des. Devel. Ther.*, **11**, 163 (2017).

(11) T. Taniguchi, Y. Iizumi, M. Watanabe, M. Masuda, M. Morita, Y. Aono, S. Toriyama, M. Oishi, W. Goi, and T. Sakai, *Cell Death Dis.*, **7** (2016).

(12) G. Wang, X. Guo, H. Chen, T. Lin, Y. Xu, Q. Chen, J. Liu, J. Zeng, X. K. Zhang, and X. Yao, *Bioorganic Med. Chem. Lett.*, **22**, 2114 (2012).

(13) J. Vanamala, L. Reddivari, S. Radhakrishnan, and C. Tarver, *BMC Cancer*, **10**, 238 (2010).

(14) Y. O. Jeon, J. S. Lee, and H. G. Lee, *Colloids Surf. B: Biointerfaces*, 147 (2016).

(15) J. Park, N. R. Kadasala, S. A. Abouelmagd, M. A. Castanares, D. S. Collins, A. Wei, and Y. Yeo, *Biomaterials*, **101**, 285 (2016).

(16) J. H. Lim, D. E. Kim, E.-J. Kim, C. D. Ahrberg, and B. G. Chung, *Macromol. Res.*, DOI: 10.1007/s13233-018-6067-3 (2018).

(17) C. Kim, S.-Y. Kim, Y. T. Lim, and T. S. Lee, *Macromol. Res.*, **25**, 572 (2017).

(18) S. V. Berwin Singh, J. Kim, H. Park, G. Khang, and D. Lee, *Macromol. Res.*, **25**, 749 (2017).

(19) C.-H. Tang and L. Shen, *J. Agric. Food Chem.*, **12**, 3097 (2013).

(20) F. Kratz, *J. Control. Release*, **132**, 171 (2008).

(21) C. He, Y. Hu, L. Yin, C. Tang, and C. Yin, *Biomaterials*, **31**, 3657 (2010).

(22) T. Osaka, T. Nakanishi, S. Shanmugam, S. Takahama, and H. Zhang, *Colloids Surf. B: Biointerfaces*, **71**, 325 (2009).

(23) H. Y. Nam, S. M. Kwon, H. Chung, S.-Y. Lee, S.-H. Kwon, H. Jeon, Y. Kim, J. H. Park, J. Kim, S. Her, Y.-K. Oh, I. C. Kwon, K. Kim, and S. Y. Jeong, *J. Control. Release*, **135**, 259 (2009).

(24) P. Anand, H. B. Nair, B. Sung, A. B. Kunnumakkara, V. R. Yadav, R. R. Tekmal, and B. B. Aggarwal, *Biochem. Pharmacol.*, **79**, 330 (2010).

(25) M. Ghorbani and H. Hamishehkar, *Int. J. Pharm.*, **520**, 126(2017).

(26) M. Ghorbani, H. Hamishehkar, N. Arsalani, and A. A. Entezami, *Mater. Sci. Eng. C*, **68**, 436 (2016).

(27) H. Andishmand, M. Tabibiazar, and M. Amin, *Int. J. Biol. Macromol.*, **97**, 16 (2017).

(28) A. Lamprecht, N. Ubrich, H. Yamamoto, U. Schäfer, H. Takeuchi, P. Maincent, Y. Kawashima, and C.-M. Lehr, *J. Pharmacol. Exp. Ther.*, **299**, 775 (2001).

(29) D. Volodkin and R. Von Klitzing, *Curr. Opin. Colloid Interface Sci.*, **19**, 25 (2014).

(30) Y. Wang, S. Xu, W. Xiong, Y. Pei, B. Li, and Y. Chen, *Colloids Surf. B: Biointerfaces*, **146**, 107 (2016).

(31) R. Weissleder, M. Nahrendorf, and M. J. Pittet, *Nat. Mater.*, **13**, 125 (2014).

(32) V. J. Mohanraj and Y. Chen, *Trop. J. Pharm. Res.*, **5**, 561 (2007).

(33) P. Jiang, D. Yu, W. Zhang, Z. Mao, C. Gao, Q. Wang, L. Wang, M. S. Detamore, C. Berkland, R. C. Mundargi, V. R. Babu, and V. Rangaswamy, *RSC Adv.*, **5**, 40924 (2015).

